

Core formation and metal–silicate fractionation of osmium and iridium from gold

James M. Brenan^{1*} and William F. McDonough²

The abundances of the highly siderophile elements as well as their relative proportions¹ in the mantle deviate from those predicted by equilibrium partitioning between metal and silicate during the formation of the Earth's core. This discrepancy is generally explained by invoking the addition of a late veneer of extraterrestrial material to the mantle after core formation was complete². Recently reported partition coefficients for gold, platinum and palladium^{3–5} could result in mantle abundances consistent with equilibrium partitioning. However, whether these results can be extrapolated to all highly siderophile elements, and thereby preclude the need for a late veneer, remains to be verified. Here we use high-temperature experiments to determine the metal–silicate partition coefficients for osmium, iridium and gold. On the basis of our estimates, equilibrium partitioning during core formation can explain the observed concentration of gold in the mantle, but not that of osmium and iridium. We conclude that not all highly siderophile elements were affected by core formation in the same way, and that the abundances of elements such as osmium and iridium require the addition of a late veneer.

During terrestrial accretion, heating from the conversion of kinetic energy of impactors and the reduction of gravitational potential probably caused widespread melting of the growing planet, separating Fe–Ni liquid from molten silicate, and removing siderophile trace elements to the proto-Earth's centre⁶. Constraints from Hf–W chronometry and numerical modelling suggest that core formation, at least at its later stages, would have involved equilibration between molten metal and silicate to the rheological base of the melted layer^{7,8}. Hence, this process should have established the siderophile element composition of the residual mantle in a manner predictable from high-pressure and -temperature laboratory measurements. Past work has ascribed the behaviour of the moderately siderophile elements (MSEs; Mo, W, Cr, V, Mn and so on) to a combination of metal extraction and accretion of compositionally distinct components^{9,10}. More recently it has been shown that, if metal–silicate partitioning is appropriately parameterized, a match to mantle MSE abundances can be achieved assuming metal–silicate equilibrium at a fixed segregation depth¹¹, or with evolving pressure, temperature and oxygen fugacity, f_{O_2} (ref. 12). However, the highly siderophile elements (HSEs: Au, Re and the platinum-group metals) are difficult to interpret in the context of equilibrium models. Most past work on HSE partitioning has been at 0.1 MPa and relatively low temperature (~1,600–1,700 K) and showed that at the relatively reduced f_{O_2} attending core formation (that is, ~2 log units more reducing than the iron–wüstite oxygen buffer; IW – 2), metal–silicate partitioning of all of the HSEs is likely to exceed 10^5 – 10^8 (for example, refs 13–15). Such results predict the quantitative removal of HSEs from the silicate mantle,

which is not observed (for example, ref. 1). This apparent lack of mantle HSE depletion (as well as certain other MSEs) is a longstanding issue in geochemistry, and has come to be known as the 'excess siderophile element problem'. Moderate to large differences in the relative mantle abundances of the HSEs are also predicted by the low-temperature partitioning data^{16,17}, in conflict with observed chondritic relative abundances¹. The osmium isotopic composition of mantle samples also indicates a time evolution with platinum/osmium and rhenium/osmium ratios matching those of chondritic meteorites^{18,19}. On the basis of a similarity between the abundance levels of gold in terrestrial lavas and lunar impact breccias, Kimura *et al.*² concluded that the HSEs in Earth's mantle were introduced by a late influx of meteoritic material, or late veneer, thus restocking the mantle inventory previously depleted by core formation.

Murthy²⁰ proposed that there should be a convergence of metal–silicate partitioning values at the very high temperatures likely during core formation (that is, >3,000 K), thus reviving the equilibrium hypothesis. Although his strategy to estimate high-temperature partitioning was shown to be flawed (for example, Capobianco *et al.*²¹, and references therein), more recent experimental work indicates that, although pressure has little effect on metal–silicate partitioning of the HSEs (refs 22, 23), increased temperature can decrease significantly the partitioning of palladium⁵, gold³ and possibly platinum (ref. 4, but see also ref. 23). Similar behaviour for the other HSEs, as required by mantle composition, has not been documented, so the veracity of the equilibrium model remains untested. Here we focus on the metal–silicate partitioning behaviour of osmium, iridium and gold, as low-temperature metal–silicate partitioning experiments document $D_{Os, Ir}$ at least $\times 1,000$ larger than D_{Au} at similar conditions of temperature and f_{O_2} (refs 13, 16, 17, 24–26). The effect of temperature on closing this gap is unknown. Combined with the data for Pt and Re, knowledge of osmium partitioning at high temperature also provides essential constraints on the likely osmium isotopic evolution of the mantle following equilibrium core separation.

The experiments used samples consisting of synthetic basalt plus a metal mixture, with most encapsulated in high-purity graphite, but we also report on carbon-free experiments done with capsules made from Fe–Ir alloy (see the Methods section and Supplementary Information for full details of experiments and their analysis; Supplementary Table S1 provides a summary of the experiments). The added metal mixture comprised Au-encapsulated osmium or iridium, or in a few cases, Fe powder mixed with 1–10 wt% of Au or Au + Os or Ir. In the former configuration, gold serves to wet Os or Ir grains, and texturally isolates them from the silicate melt. We believe this configuration inhibits Os or Ir nugget formation, which we have found to be a pernicious aspect of experiments containing

¹Department of Geology, University of Toronto, Toronto, Canada M5S 3B1, ²Department of Geology, University of Maryland, College Park, Maryland 20742, USA. *e-mail: brenan@geology.utoronto.ca.

these elements. However, both Ir and Os are sparingly soluble in molten Au (see Supplementary Table S3), which allows for efficient metal–silicate chemical exchange. Experiments were done at temperatures of 2,173–2,588 K, at a fixed pressure of 2 GPa, using a piston–cylinder apparatus and using standard techniques. The amount of Fe dissolved in Au coexisting with FeO-bearing molten silicate was used to calculate f_{O_2} , which is expressed here relative to the iron–wüstite buffer. Run products were analysed for major elements by electron microprobe, and trace elements by laser-ablation inductively coupled plasma mass spectrometry (ICP-MS). Time-resolved spectra obtained for glasses from experiments that were initially metal undersaturated show a uniform distribution of Os, Ir and Au, consistent with homogeneous solution of these elements in the silicate melt (see Supplementary Fig. S1). We assessed equilibrium in our experiments by approaching metal solubilities from both over- and undersaturated conditions. Major and trace element abundances in the silicate and metal phases are provided in Supplementary Tables S2 and S3.

For experiments in which Os, Ir and Au are dilute in the Fe alloy, values of $D^{\text{metal/silicate}}$ are calculated directly from the ratio of concentrations in the coexisting metal and silicate phases. In the case of experiments containing nearly pure Os, Ir and Au, metal–silicate partition coefficients are calculated using the silicate melt concentrations of these elements, corrected for the activity of Os, Ir or Au in the coexisting metal, and accounting for the change in Os, Ir or Au activity following dilution in Fe metal²⁷ (equation (1); see the Methods section and Supplementary Information for details). Metal–silicate partition coefficients are provided in Supplementary Table S2. Figure 1 shows metal–silicate partition coefficients for Os, Ir and Au as a function of temperature from this and previous studies. Here we show results from experiments done at nearly the same relative f_{O_2} of $\sim\text{IW} + 2$ (except for the experiments of ref. 26 done at $\text{IW} + 4$; see the Methods section for specific values of relative f_{O_2} from previous work). The lines in Fig. 1 were calculated by weighted least-squares linear regression of the partitioning data measured in this study, and fit parameters are provided in the Methods section (equations (2)–(4)). The slopes of $\log D^{\text{metal/silicate}}$ versus temperature yield indistinguishable values with a $\sim 10^4$ offset in partitioning for Os and Ir versus that of Au. Whereas metal–silicate partitioning for Au at high temperature and 2 GPa approaches values required to reproduce mantle abundances, that for Os and Ir results in quantitative removal of these elements from the silicate melt. Experimental results for Os partitioning at low pressure (0.1 MPa) plot below the low-temperature extrapolation of our data, implying that the effect of pressure may be to increase metal–silicate partitioning of this element, thus increasing the Au–Os partitioning offset. However, glass concentrations from two of the low-pressure studies^{24,25} were measured using bulk techniques, so it is possible that their partitioning values are underestimated because of micronugget contamination. Although experiments were done at a more oxidized f_{O_2} than expected for core formation ($\text{IW} + 4$), partition coefficients derived from the solubility data of Brenan *et al.*²⁶ represent minimum values, as the Os content of the run-product glass was undetectable, as determined by laser-ablation ICP-MS analysis. Lower temperature values of Ir partitioning are nearly the same or higher than the extrapolation of our (limited) high-temperature data. This finding implies that pressure may lower slightly the metal–silicate partitioning of this element. However, low-temperature partitioning values can be subject to considerable uncertainty, as they are derived from solubility data extrapolated from higher f_{O_2} , assuming a 2^+ oxidation state; such low- f_{O_2} experiments are subject to contamination from undissolved iridium micronuggets. Nonetheless, these data are our best estimates, in lieu of direct measurements. Previous measurements of the metal–silicate partitioning for Au at similar

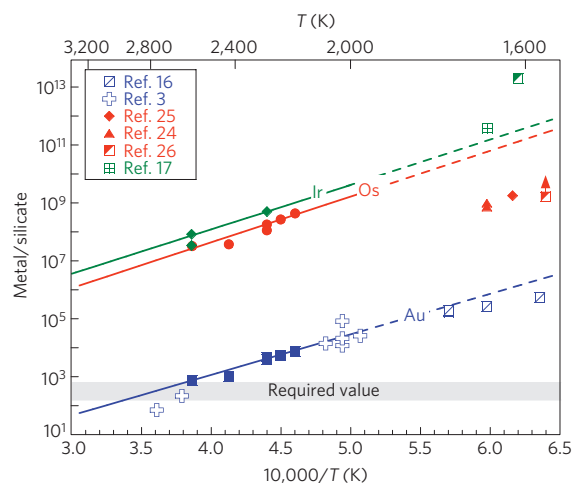


Figure 1 | Metal–silicate partition coefficients as a function of inverse absolute temperature. Values are shown for osmium, iridium and gold calculated from the solubility experiments of this study (filled red circles, blue squares and green diamonds) done at 2 GPa and relative f_{O_2} of $\sim\text{IW} + 2$. Other results are from experiments either done at or extrapolated to similar relative f_{O_2} (except for the experiments of ref. 26 done at $\text{IW} + 4$; see the Methods section for specific values of relative f_{O_2} from previous work). The data points with the upward-pointing arrows are minimum values corresponding to experiments in which the metal concentration in the silicate glass is below detection. ‘Required value’ corresponds to the metal–silicate partition coefficient necessary to account for the abundances of these elements in the primitive upper mantle. The error bars are 1σ based on the variation in multiple analyses.

relative f_{O_2} , but different pressures (0.1 MPa–23 GPa; refs 3, 16), show good agreement with our results, despite significant down-temperature extrapolation. This lack of a pressure effect is also consistent with the previous results for Pt and Pd (refs 22, 23), highlighting temperature as a significant variable to control metal–silicate partitioning.

Figure 2 shows the effect of f_{O_2} on the metal–silicate partitioning of Au, Os and Ir determined at 2,273 and 2,588 K. Data for Os and Ir show a general increase in partitioning with decreasing f_{O_2} , consistent with solution of both metals as an oxide species in the silicate melt (probably as 1^+ for Ir and mixed 1^+ and 2^+ for Os; see Supplementary Information). Partition coefficients for Au show a slight drop with decreasing f_{O_2} , with similar behaviour observed in experiments done at 0.1 MPa and low f_{O_2} (ref. 16). This result is consistent with Au solution in molten silicate as a mixture of Au^0 and AuSi_x species, although carbonyl species cannot be excluded for experiments done in graphite (see Supplementary Information for discussion). At 2,588 K and $\text{IW} - 1.5$, which is the lowest f_{O_2} of our study, and only ~ 0.5 log units more oxidized than likely core-forming conditions, the metal–silicate partition coefficient for Au is ~ 300 , whereas the minimum value for both Os and Ir measured in the same experiments is $\sim 10^7$, indicating a minimum difference in partitioning of $\sim 10^4$. Experiments done in graphite and Fe–Ir capsules yield similar partition coefficients, indicating that the presence of dissolved carbon has a negligible effect on this result.

In combination with data from the literature, our results also constrain the expected osmium isotopic evolution of the mantle following equilibrium core formation. Ohtani and Yurimoto²⁸ determined $D^{\text{metal-silicate}}$ for Re of 440 at 20 GPa, 2,773 K and $\text{IW} - 1.2$, which allows an assessment of the Re/Os ratio imparted to the silicate Earth by metal–silicate equilibrium. Extrapolating our results from experiments done at $\text{IW} + 2$ to 2,773 K, yields $D^{\text{metal-silicate}}$ for Os of 1×10^7 , yielding a minimum Re/Os ratio for

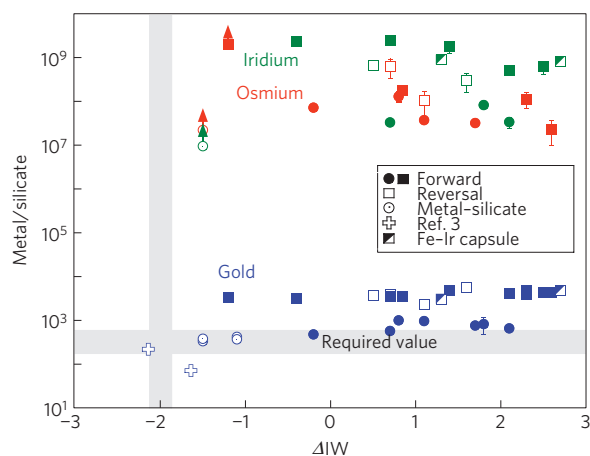


Figure 2 | Metal-silicate partition coefficients as a function of oxygen fugacity. Values are shown for osmium, iridium and gold as a function of the f_{O_2} relative to the iron-wustite (I-W) equilibrium. Filled squares and circles correspond to experiments done at 2,273 K and 2,588 K, respectively. Most partition coefficients are calculated from the solubility of the pure metal, but data denoted as ‘metal-silicate’ are direct determinations from experiments using an iron-rich metal phase (including the experiments of Danielson *et al.*³). Reversal experiments were done by saturating the silicate melt at 2,588 K, then re-equilibration at 2,273 K, in which the metal solubility is lower. Most experiments were encapsulated in graphite. The effect of dissolved carbon on metal-silicate partitioning was determined from experiments encapsulated in Fe-Ir alloy. Similar results for either capsule material indicate a negligible effect of carbon on partitioning behaviour. For details on the data points with upward-pointing arrows, ‘Required value’ and the error bars, see Fig. 1 caption.

the silicate Earth of $\sim 1,900$, grossly higher than the value of 0.096 ($\pm 2\%$) required by $^{187}\text{Os}/^{188}\text{Os}$ systematics¹⁸. Although we have not determined the temperature dependence of Os partitioning at more reducing conditions, we expect it to be similar to behaviour at higher f_{O_2} , but with $D^{\text{metal/silicate}}$ for Os shifted to larger values. Thus, the estimated suprachondritic Re/Os ratio is probably a minimum value. Estimates of the Pt/Os imparted to the silicate Earth differ, depending on the chosen data set for Pt partitioning. Whereas Ertel *et al.*²³ predict $D^{\text{metal/silicate}}$ for Pt to be similar to our Os data at high T and low f_{O_2} , values measured by Cottrell and Walker⁴ are 2–3 orders of magnitude lower at similar conditions, with the latter study implying a significantly suprachondritic evolution in $^{186}\text{Os}/^{188}\text{Os}$, which is not permissible.

Our partitioning results for Os and Ir indicate that neither the effects of temperature nor f_{O_2} on metal-silicate partitioning can account for the ‘excess’ of osmium and iridium in the silicate Earth. The observed osmium isotopic evolution of the mantle is also inconsistent with the expected imprint of metal-silicate equilibrium. Our data for Au partitioning, in contrast, indicate that high-temperature metal-silicate equilibrium can account for mantle abundances of this element, similar to recent results obtained for palladium⁵. The delivery of a small amount of exogenous chondritic component (estimated at $\sim 0.5\%$) to the mantle after core formation provides a way to overcome the imbalance in osmium and iridium abundances imparted by metal-silicate equilibrium^{2,9,10}. This holds true for other elements that had been similarly depleted (for example, S, Se, Te; ref. 29). Such additions would also provide gold and palladium to a mantle only mildly impoverished in these elements, thus accounting for their slight (twofold) overabundance in the mantle relative to chondritic values¹. Additions of such small amounts of an HSE component would have a negligible impact on the much higher levels of the MSEs, which had

been established by either metal-silicate equilibrium^{11,12} or a combination of processes^{9,10}.

Methods

Samples consisted of synthetic basalt plus a metal mixture, encapsulated in either high-purity graphite or in some cases Fe-Ir alloy (fabricated from pressed then sintered metal powder mixtures). The synthetic basalt was initially prepared Fe-free, with different proportions of FeO and Fe_2O_3 (as well as Si metal in some cases) added so as to adjust the final f_{O_2} of the experiment. Experiments were done using a piston-cylinder apparatus using a 1.27-cm-bore pressure vessel with pressure cells consisting of sintered MgO filler pieces and a graphite furnace fitted into sleeves of soft-sintered barium carbonate. All experiments were done at a confining pressure of 2 GPa, and terminated by cutting power to the furnace. Quenched run products consisted of water/clear silicate glass and a composite metal bead, consisting of texturally homogeneous Ir or Os grains surrounded by dendritic gold. In a few cases, the silicate glass had begun to quench crystallize on the alloy bead or walls of the capsule, and in the highest-temperature experiments, small bubbles were present with adhering gold alloy grains (see Supplementary Information for more details).

Run products were mounted in epoxy, then ground and polished for textural and elemental analysis. Major element analysis was carried out using the Cameca SX50 electron microprobe at the University of Toronto. The trace element content of run-product glasses was determined using the laser-ablation ICP-MS facilities in the Departments of Geology at the University of Maryland and at University of Toronto. Both systems use a frequency-quintupled Nd:YAG laser operating at 213 nm, coupled to either an Element 2 (ThermoElectron) magnetic sector ICP-MS (Maryland) or a VG PQExcell quadrupole ICP-MS (Toronto) with He flushing the ablation cell. Analyses were obtained using a laser fluence of $\sim 2 \text{ J cm}^{-2}$, a repetition rate of 10 Hz and a spot size of 100–200 μm . Factory-supplied time-resolved software was used for the acquisition of individual analyses. A typical analysis involved 20 s of background acquisition with the ablation cell being flushed with He, followed by laser ablation for 60 s. Analyses were collected in a sequence, with the first and last four spectra acquired on sulphide and glass standard reference materials (see Supplementary Information for details of the standards used). Data reduction was carried out using either LAMTRACE (Maryland) or GLITTER (Toronto) version 5.3 software package, supplied by Macquarie Research. Ca was used as the reference element to correct for ablation yields in silicate glass and this method also provided precise Ni data used to correct ablation yields when using the sulphide standard. Where possible, multiple isotopes were measured for each element, yielding identical concentrations, indicating the lack of interfering species. Summaries of glass and alloy compositions are provided in Supplementary Tables S2 and S3, respectively.

For experiments in which Os and Au are dilute in the Fe alloy, values of $D^{\text{metal/silicate}}$ are calculated directly from the ratio of concentrations in the coexisting phases. In the case of experiments containing nearly pure Os, Ir and Au, metal-silicate partition coefficients are calculated by accounting for the change in Os, Ir or Au activity following dilution in Fe metal. We use the relation derived by Borisov *et al.*²⁷:

$$D^{\text{metal/silicate}} = \frac{1}{AC^{\text{metal}}(\text{sil})\gamma_{\text{metal}}^{\text{Fe}}} \quad (1)$$

in which A is a mole-to-weight conversion factor, $C^{\text{metal}}(\text{sil})$ is the concentration of the metal in silicate melt when the activity of the metal phase is one and $\gamma_{\text{metal}}^{\text{Fe}}$ is the activity coefficient of the metal at infinite dilution in liquid Fe. The temperature dependence of metal-silicate partitioning was fitted to the appropriate form by the method of weighted least-squares, yielding the following expressions:

$$\log D_{\text{Os}} = 1.32(0.41) + [1.58(0.09) \times 10^4]/T \text{ (K)} \quad (2)$$

$$\log D_{\text{Ir}} = 1.96(1.56) + [1.53(0.38) \times 10^4]/T \text{ (K)} \quad (3)$$

$$\log D_{\text{Au}} = -2.53(1.09) + [1.40(0.24) \times 10^4]/T \text{ (K)} \quad (4)$$

Further Au partitioning values plotted in Fig. 1 are from Danielson *et al.*³, done at pressures of 3–23 GPa and f_{O_2} of IW – 1.2 to –2.45, and calculated from the gold solubility measurements of Borisov and Palme¹⁶ done at a pressure of 0.1 MPa and $\sim \text{IW} + 2$. Other partitioning values for osmium are calculated from 0.1 MPa metal solubility data^{24–26}. Yokoyama *et al.*³⁰ recently obtained a metal-silicate partition coefficient for Os of $> 2.5 \times 10^5$ at 2 GPa and 2,673 K (not shown), which is consistent with our results. Partitioning values for iridium are calculated by extrapolating the 0.1 MPa solubility data^{17,26} to an f_{O_2} of IW + 2 (also consistent with the results of ref. 13). In this case, only values measured under oxidizing conditions were used to extrapolate, and a 2^+ oxidation state is assumed for the dissolved Ir species in the silicate melt.

Received 23 April 2009; accepted 18 September 2009;
published online 18 October 2009

References

1. Becker, H. *et al.* Highly siderophile element composition of the Earth's primitive mantle: Constraints from new data on peridotite massifs and mantle xenoliths. *Geochim. Cosmochim. Acta* **70**, 4528–4550 (2006).
2. Kimura, K., Lewis, R. S. & Anders, E. Distribution of gold and rhenium between nickel–iron and silicate melts: Implications for the abundance of siderophile elements on the Earth and Moon. *Geochim. Cosmochim. Acta* **38**, 683–701 (1974).
3. Danielson, L., Sharp, T. & Hervig, R. L. *36th Lunar and Planetary Science Conference Abstr.* 1955 (Lunar and Planetary Institute, 2005).
4. Cottrell, E. & Walker, D. Constraints on core formation from Pt partitioning in mafic silicate liquids at high temperatures. *Geochim. Cosmochim. Acta* **70**, 1565–1580 (2006).
5. Righter, K., Humayun, M. & Danielson, L. Partitioning of palladium at high pressures and temperatures during core formation. *Nature Geosci.* **1**, 321–323 (2008).
6. Rubie, D. C., Nimmo, F. & Melosh, H. J. Formation of Earth's core. *Treatise on Geophys.* **9**, 51–90 (2007).
7. Rubie, D.C. *et al.* Mechanisms of metal–silicate equilibration in the terrestrial magma ocean. *Earth Planet. Sci. Lett.* **205**, 239–255 (2003).
8. Nimmo, F. & Agnor, C. B. Isotopic outcomes of N-body accretion simulations: Constraints on equilibration processes during large impacts from Hf–W observations. *Earth Planet. Sci. Lett.* **243**, 26–43 (2006).
9. Wanke, H. & Dreibus, G. Chemical composition and accretion history of terrestrial planets. *Phil. Trans. R. Soc. A* **325**, 545–557 (1988).
10. O'Neill, H. St. C. The origin of the Moon and the early history of the Earth—a chemical model. Part 2: The Earth. *Geochim. Cosmochim. Acta* **55**, 1159–1172 (1991).
11. Righter, K., Drake, M. J. & Yaxley, G. Prediction of siderophile element metal/silicate partition coefficients to 20 GPa and 2800 °C: The effects of pressure, temperature, oxygen fugacity and silicate melt and metallic melt compositions. *Phys. Earth Planet. Inter.* **100**, 115–134 (1997).
12. Wood, B. J., Walter, M. J. & Wade, J. Accretion of the Earth and segregation of its core. *Nature* **441**, 825–833 (2006).
13. Borisov, A. & Palme, H. Solubility of iridium in silicate melts: New data from experiments with Ir₁₀Pt₉₀ alloys. *Geochim. Cosmochim. Acta* **59**, 481–485 (1995).
14. Ertel, W. *et al.* Solubilities of Pt and Rh in haplobasaltic silicate melt at 1300 °C. *Geochim. Cosmochim. Acta* **63**, 2439–2449 (1999).
15. Ertel, W. *et al.* The solubility of rhenium in silicate melts: Implications for the geochemical properties of rhenium at high temperatures. *Geochim. Cosmochim. Acta* **65**, 2161–2170 (2001).
16. Borisov, A. & Palme, H. Experimental determination of the solubility of Au in silicate melts. *Mineral. Petrol.* **56**, 297–312 (1996).
17. O'Neill, H. St. C. *et al.* Experimental petrochemistry of some high siderophile elements at high temperatures and some implications for core formation and the mantle's early history. *Chem. Geol.* **120**, 255–273 (1995).
18. Meisel, T. *et al.* Osmium isotopic compositions of mantle xenoliths: A global perspective. *Geochim. Cosmochim. Acta* **65**, 1311–1323 (2001).
19. Brandon, A. D., Walker, R. J. & Puchtel, I. S. Platinum–osmium isotope evolution of the Earth's mantle: Constraints from chondrites and Os-rich alloys. *Geochim. Cosmochim. Acta* **70**, 2093–2103 (2006).
20. Murthy, V. R. Early differentiation of the Earth and the problem of mantle siderophile elements: A new approach. *Science* **253**, 303–306 (1991).
21. Capobianco, C. J., Jones, J. H. & Drake, M. J. Metal–silicate thermochemistry at high temperature—magma oceans and the excess siderophile problem of the Earth's upper mantle. *J. Geophys. Res.* **98**, 5433–5443 (1993).
22. Holzheid, A. *et al.* Evidence for a late chondritic veneer in the Earth's mantle from high pressure partitioning of palladium and platinum. *Nature* **406**, 396–399 (2000).
23. Ertel, W. *et al.* Experimental study of platinum solubility in silicate melt to 14 GPa and 2273 K: Implications for accretion and core formation in Earth. *Geochim. Cosmochim. Acta* **70**, 2591–2602 (2006).
24. Borisov, A. & Walker, R. J. Os solubility in silicate melts: New efforts and results. *Am. Mineral.* **85**, 912–917 (2000).
25. Fortenfant, S. S. *et al.* Oxygen fugacity dependence of Os solubility in haplobasaltic melts. *Geochim. Cosmochim. Acta* **70**, 742–756 (2006).
26. Brennan, J. M., McDonough, W. F. & Ash, R. An experimental study of the solubility and partitioning of iridium, osmium and gold between olivine and silicate melt. *Earth Planet. Sci. Lett.* **237**, 855–872 (2005).
27. Borisov, A., Palme, H. & Spettel, B. Solubility of palladium in silicate melts: Implications for core formation in the earth. *Geochim. Cosmochim. Acta* **58**, 705–716 (1994).
28. Ohtani, E. & Yurimoto, H. Element partitioning between metallic liquid, magnesiowustite and silicate liquid at 20 GPa and 2500 °C: A secondary ion mass spectrometric study. *Geophys. Res. Lett.* **23**, 1993–1996 (1996).
29. Rose, L. A. *et al.* Effect of pressure, temperature and oxygen fugacity on the metal–silicate partitioning of Te, Se, and S: Implications for earth differentiation. *Geochim. Cosmochim. Acta* **73**, 4598–4615 (2009).
30. Yokoyama, T. *et al.* Low osmium solubility in silicate at high pressures and temperatures. *Earth Planet. Sci. Lett.* **279**, 165–173 (2009).

Acknowledgements

J.M.B. gratefully acknowledges research and facilities support from the Natural Sciences and Engineering Research Council of Canada. W.F.M. gratefully acknowledges support from NASA Cosmochemistry grant NNX08AH76G and NSF grant No. 0739006. We are grateful to R. Ash for help with some of the laser-ablation analyses.

Author contributions

J.M.B. carried out the experiments, and acquired the major element and some of the trace element data. W.F.M. acquired most of the trace element data. Both authors contributed to the research, data interpretation and manuscript preparation.

Additional information

Supplementary information accompanies this paper on www.nature.com/naturegeoscience. Reprints and permissions information is available online at <http://npg.nature.com/reprintsandpermissions>. Correspondence and requests for materials should be addressed to J.M.B.